Materials Advances

ROYAL SOCIETY OF CHEMISTRY

PAPER

View Article Online
View Journal | View Issue

Cite this: *Mater. Adv.*, 2024, 5, 5244

Improving high efficiency and device lifetime of blue emitters with 3*H*-benzo[*cd*]pyrene core and optimized bulky side groups†

Hyukmin Kwon, Sunwoo Park, Seokwoo Kang, Sangwook Park, Kiho Lee, Hayoon Lee and Jongwook Park *

Received 1st May 2024,
Accepted 9th May 2024

DOI: 10.1039/d4ma00452c

rsc.li/materials-advances

We designed and synthesized two blue fluorescent dopants, *N*1,*N*7-bis(4-(*tert*-butyl)-2,6-dimethylphenyl)-9-isopropyl-5,5-dimethyl-*N*1,*N*7-diphenyl-4,5,6*a*1,11*a*1-tetrahydro-3*H*-benzo[*cd*]pyrene-1,7-diamine (DMP-BP) and *N*1,*N*7-bis(dibenzo[*b*,*d*]furan-4-yl)-9-isopropyl-*N*1,*N*7-bis(4-isopropylphenyl)-5,5-dimethyl-4,5-dihydro-3*H*-benzo[*cd*]pyrene-1,7-diamine (DBF-BP), by introducing alkylated *N*-phenylaniline and alkylated dibenzo[*b*,*d*]furan-amine as side groups, based on the pyrene chromophore, 3*H*-benzo[*cd*]pyrene (BP) core. When used as dopants in OLED devices, both DMP-BP and DBF-BP exhibited device performances with current efficiencies of over 9 cd A^{-1} and full width at half maximum (FWHM) values of less than 44 nm. Both materials achieved an excellent device lifetime with LT95 values exceeding 200 hours. Particularly, the DBF-BP device demonstrated a maximum external quantum efficiency of 8.03% and an EL spectrum with a narrow FWHM of 42 nm. The LT_{95} lifetime of the DBF-BP device was 207 hours, corresponding to an outstanding device lifetime of over 12 000 hours when extrapolated to LT_{50}.

Introduction

Since its initial development by Tang and VanSlyke in 1987, organic light-emitting diodes (OLEDs) have garnered continuous interest from both academic researchers and industrial sectors. This technology has been particularly applied to full-color displays like mobile phones and TVs. To commercialize full-color OLED displays, it is essential to develop red, green, and blue emitters with high electroluminescence (EL) efficiency, a wide color gamut, and long device lifetimes.[1–4] Generally, luminescent materials are categorized into fluorescence and phosphorescence based on their luminescence mechanisms. In principle, fluorescence has an internal quantum efficiency of only 25%, while phosphorescence exhibits an internal quantum efficiency of 100%.[5] However, phosphorescent emitters have relative challenges in implementing a wide bandgap due to their mechanism, especially in the case of blue-emitting materials. Furthermore, blue phosphorescent organic light-emitting diodes suffer from efficiency roll-off issues at high current density and exhibit a short device lifetime at high luminescence.[6,7] Therefore, research on blue fluorescence materials continues to be actively pursued to overcome the challenges associated with blue phosphorescent emitters.[8–10] Nonetheless, the performance of blue-emitting materials remains inferior to that of red and green materials, making the development of high-efficiency and long-lifetime blue-emitting materials a crucial task.[11–13] In the scope of blue-emitting materials, chromophores such as anthracene, pyrene, and chrysene are well-known as blue fluorescence chromophores.[14–16] Among these, pyrene has attracted significant attention in the field of organic electronic devices due to its excellent electronic and photophysical properties as a polycyclic aromatic hydrocarbon composed of four fused benzene rings.[17–19] Pyrene, characterized by its extended π-conjugation, exhibits strong absorption in the ultraviolet-visible (UV-Vis) region, leading to efficient luminescence in the visible region. Moreover, its fluorescence characteristics in the deep blue region, combined with high thermal stability and excellent photostability, have received significant attention.[20,21] These characteristics fulfill the requirements for a blue-emitting material to achieve full-color displays with high efficiency and longevity. However, pyrene presents challenges such as molecular aggregation-induced quenching (AIQ) and excimer formation due to its planar structural characteristics.[22–24] In this regard, various strategies for designing pyrene derivatives have been reported to prevent intermolecular packing.[25–27] In this study, we developed a novel core and side group simultaneously based on the core-side concept, aiming to minimize intermolecular packing. First, we selected a 3*H*-benzo[*c*,*d*]pyrene (BP) core with high photoluminescence quantum yield (PLQY) as the core. The BP core incorporates aliphatic cyclic groups and alkyl groups to preserve the

Integrated Engineering, Department of Chemical Engineering, Kyung Hee University, Gyeonggi, 17104, Republic of Korea. E-mail: jongpark@khu.ac.kr

† Electronic supplementary information (ESI) available. See DOI: https://doi.org/10.1039/d4ma00452c

conjugation length of pyrene while minimizing their influence on the electron density. Here, pyrene-based blue fluorescent dopant materials by introducing bulky and electron-donating alkylated *N*-phenylaniline and alkylated dibenzo[*b*,*d*]furan-amine as side groups were designed. Specifically, we synthesized *N*1,*N*7-bis(4-(*tert*-butyl)-2,6-dimethylphenyl)-9-isopropyl-5,5-dimethyl-*N*1,*N*7-diphenyl-4,5,6*a*1,11*a*1-tetrahydro-3*H*-benzo[*cd*]pyrene-1,7-diamine (DMP-BP) and *N*1,*N*7-bis(dibenzo[*b*,*d*]furan-4-yl)-9-isopropyl-*N*1,*N*7-bis(4-isopropylphenyl)-5,5-dimethyl-4,5-dihydro-3*H*-benzo[*cd*]pyrene-1,7-diamine (DBF-BP). To efficiently prevent intermolecular packing and enhance EL performance, various sizes of alkyl groups were substituted at multiple positions of the side group. Additionally, in the case of DBF-BP, a bulky dibenzofuran group with an electron-donating effect was introduced into the side group, simultaneously increasing the size and electron-donating characteristics of the side group.[28] These two materials were applied to OLED devices, confirming excellent EL performance and long device lifetime.

Result and discussion

Molecular design, synthesis, and characterization

The pyrene chromophore has been widely utilized as a core group in organic light-emitting materials due to its high luminescence efficiency and stability. In this study, a novel chromophore, 3*H*-benzo[*cd*]pyrene (BP) core, based on the pyrene chromophore, was designed and synthesized by introducing various alkyl groups as side groups. Previously, Suh group reported DI-1,6-DAP as a blue-emitting luminophore by introducing isopropyl groups at the 3rd and 8th positions of the pyrene chromophore and utilizing *N*-phenylnaphthalene-1-amine as a side group.[26] DI-1,6-DAP exhibited a maximum photoluminescence value of 459 nm and a full width at half maximum (FWHM) value of 54 nm in solution state, along with a maximum current efficiency (CE) of 6.89 cd A^{-1} and a maximum external quantum efficiency (EQE) of 5.45%. In this study, molecular structures were designed and synthesized to obtain two blue-fluorescent dopant materials, DMP-BP and DBF-BP, using a pyrene-based novel BP core (Fig. 1 and Scheme S1, ESI†). These materials were substituted with alkylated *N*-phenylaniline and alkylated dibenzo[*b*,*d*]furan-amine as side groups, respectively, to effectively suppress intermolecular packing and interactions. Furthermore, various alkyl groups such as methyl, isopropyl, and *tert*-butyl were introduced as side groups, along with the incorporation of bulky moieties like dibenzofuran. These molecular design strategies may be advantageous in achieving narrow FWHM, high color purity, and high luminous efficiency. The BP core, derived from the pyrene chromophore, features cyclization at positions 3 and 4 to enhance the molecular rigidity and oscillator strength, thereby reducing non-radiative decay and expecting a high photoluminescence quantum yield (PLQY) along with enhanced thermal stability. Additionally, dimethyl and isopropyl groups were introduced at positions 5 and 9 of the BP core to create a planar structure that would prevent excimer formation by inhibiting intermolecular packing compared to pyrene. The side group of DMP-BP consists of a diphenylamine derivative, with a *tert*-butyl group at the 4th position of one phenyl and methyl groups at the 2nd and 6th positions. DBF-BP utilizes an isopropyl group at the 4th position of one phenyl ring, similar to DMP-BP, and replaces the other phenyl group with a bulky dibenzofuran group with an electron-donating effect. The synthesized compounds were characterized using nuclear magnetic resonance (NMR) spectroscopy, mass spectroscopy, and elemental analysis (Fig. S1 and S2, ESI†). Further details regarding the synthesis methods are provided in the experimental section.

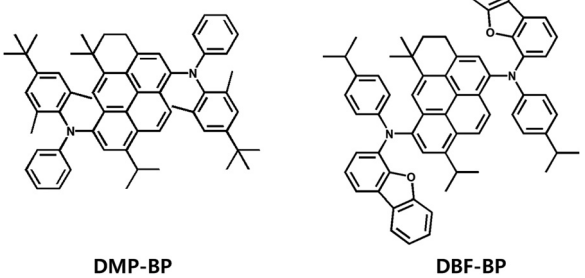

Fig. 1 Chemical structures of the 3*H*-benzo[*cd*]pyrene derivatives.

Photophysical properties

To investigate the photophysical properties of the newly synthesized BP derivatives as dopants, UV-Visible (UV-Vis) absorbance and photoluminescence (PL) spectra were measured in the solution state (Fig. 2). Table 1 summarizes the optical properties, absolute photoluminescence quantum yield (PLQY), and photophysical characteristics of the synthesized compounds. In the solution state, the UV-Vis maximum absorbance (UV_{max}) peaks of DMP-BP were observed at wavelengths of 412 nm and 435 nm, while DBF-BP showed UV_{max} at 317 nm and 422 nm. The absorbance peak at 317 nm for DBF-BP is attributed to the n–π* transition of the DBF moiety, indicating electron transition from non-bonding electron on the oxygen atom of DBF to π* level.[29] The absorption bands in the range of 350–450 nm are associated with intramolecular charge transfer (ICT) from the donor (DBF) to the acceptor (BP).[30] As shown in Fig. 2, the photoluminescence maximum wavelengths (PL_{max}) for both DMP-BP and DBF-BP were identical at 456 nm. Additionally, the full width of half-maximum (FWHM) values for DMP-BP

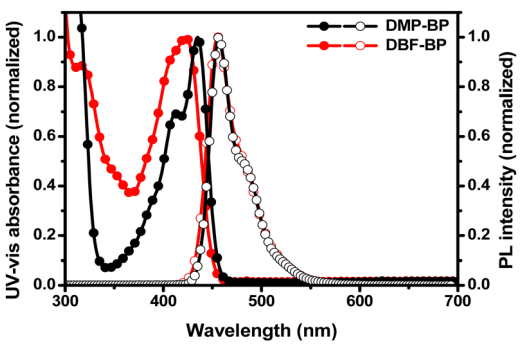

Fig. 2 UV-Vis absorption and PL spectra of 3*H*-benzo[*cd*]pyrene derivatives in solution state (toluene, 1×10^{-5} M).

Table 1 Photophysical properties of the synthesized materials

	Solution[a]				Neat film[b]						
	λ_{abs} (nm)	λ_{PL} (nm)	FWHM (nm)	PLQY (%)	λ_{abs} (nm)	λ_{PL} (nm)	FWHM (nm)	τ_F[a] (ns)	k_{rad}[c] $\times 10^8$ s^{-1}	k_{nr}[c] $\times 10^7$ s^{-1}	k_{rad}/k_{nr}
DMP-BP	412, 435	457	35	65.3	313, 413, 437	467, 495	98	2.3	2.84	15.1	1.89
DBF-BP	317, 422	457	38	65.6	430	465	61	2.2	2.98	15.7	1.90

[a] Toluene solution (1.0×10^{-5} M). [b] 4 wt% DMP-BP and DBF-BP in α,β-ADN host doped films. [c] Values of k_{rad} and k_{nr} were calculated according to the equations $k_{rad} = \Phi_F/\tau_F$ and $k_{nr} = (1/\tau_F) - k_{rad}$.

and DBF-BP were 35 nm and 38 nm, indicating similar PL spectra. This suggests that the substitution of side groups did not significantly change the molecular conjugation length. Fig. S3 (ESI†) shows that DMP-BP exhibited UV_{max} values at 313 nm, 413 nm, and 437 nm, with PL_{max} values at 467 nm and 495 nm in the film state. For DBF-BP, UV_{max} values were observed at 430 nm, with PL_{max} at 465 nm. The emission above 495 nm for DMP-BP is attributed to excimer emission, resulting in a broad shape with an FWHM value of 98 nm. In contrast, DBF-BP showed a narrower spectrum with an FWHM value of 61 nm, 37 nm narrower than DMP-BP (Fig. S3, ESI† and Table 1). To investigate the excimer characteristics of DMP-BP, additional photoluminescence (PL) measurements were conducted at concentrations ranging from 1×10^{-5} M to 1×10^{-2} M. As shown in Fig. S4 (ESI†), both materials exhibit a shift of PL_{max} towards longer wavelengths with increasing concentration. This phenomenon is attributed to the increased molecular interactions resulting from the closer proximity of molecules, which is a common observed. However, it was observed that as the concentration of DMP-BP increased, an excimer peak around 500 nm emerged, which was particularly pronounced in the film state. Consequently, through optical properties, it was confirmed that the dibenzofuran group included in the side group of DBF-BP, with its bulky structure, effectively prevents intermolecular packing and thus represents a relatively superior side group capable of achieving a narrow spectrum. To investigate the optical properties resulting from the introduction of electron-donating groups into the BP core structure, solvatochromism experiments were conducted (Fig. S5, ESI†). The solvents used in the solvatochromism experiments were toluene (dielectric constant, ε: 2.38), ethyl acetate (ε: 6.02), dichloromethane (ε: 8.93), and dimethyl sulfoxide (DMSO) (ε: 46.7). Depending on the solvent, both compounds exhibited nearly identical UV-Vis spectra shapes. As the solvent polarity increased, DMP-BP emitted light at 456, 457, 460, and 466 nm, showing a maximum red shift of up to 10 nm, while DBF-BP emitted light at 456, 456, 462, and 470 nm, exhibiting a 14 nm red shift. As solvent polarity increased, the PL emission shifted to longer wavelengths. This is because in ground states, the molecular dipole moments are not influenced by solvent polarity, thus showing similar absorption peaks. However, in excited states, the molecules are influenced by both the charge generated within the molecule and the polarity of the solvent. Consequently, as the dielectric constant of the solvent increases, molecules interact more with the solvent dipoles, stabilizing the excited state and reducing the band gap, leading to a gradual red-shift in PL_{max} values.[31] Through this red shift analysis, it was confirmed that the electron-donating effect of the side group in DBF-BP is slightly stronger. To further investigate the triplet excited states (T_1), emissions were measured at 77 K. As shown in Fig. S6 (ESI†), despite increasing the delay time from 0 ms to 150 ms, fluorescence and phosphorescence did not separate. For DMP-BP, phosphorescence emission was observed at 520 nm, and for DBF-BP, it was observed at 527 nm. Singlet excited states (S_1) and T_1 were calculated based on the maximum peak of fluorescence and phosphorescence emissions.[32] For DMP-BP, S_1 and T_1 were 2.72 and 2.39 eV, respectively, showing a ΔE_{ST} of 0.33 eV. For DBF-BP, S_1 and T_1 were 2.71 and 2.35 eV, respectively, with a ΔE_{ST} of 0.36 eV. The radiative (k_{rad}) and nonradiative rate constants (k_{nr}) for both compounds were calculated based on fluorescence lifetime measurements (Fig. S7, ESI†). The fluorescence lifetimes for DMP-BP and DBF-BP were 2.3 and 2.2 ns. The k_{rad} values were 2.84×10^8 s^{-1} and 2.98×10^8 s^{-1}, while k_{nr} values were 15.1×10^7 s^{-1} and 15.7×10^7 s^{-1} for DMP-BP and DBF-BP, respectively (Table 1). Consequently, the k_{rad}/k_{nr} values for DMP-BP and DBF-BP were found to be 1.89 and 1.90, respectively, indicating similar photophysical characteristics. Therefore, the photoluminescence quantum yield (PLQY) values of DMP-BP and DBF-BP in the solution state were also similar at 65.3% and 65.6%. The highest occupied molecular orbital (HOMO) levels for both compounds were measured using AC-2, and the lowest unoccupied molecular orbital (LUMO) levels were determined through the HOMO level and optical band gap. The optical band gap was derived from the $(h\nu)$ *versus* $(\alpha h\nu)^2$ plot by determining the absorbance edge, where α, h, and ν represent absorbance, Planck's constant, and the frequency of light, respectively. The HOMO and LUMO levels of DMP-BP and DBF-BP were −5.24 eV and −2.54 eV, −5.36 eV and −2.69 eV, respectively, with band gaps of 2.70 eV and 2.69 eV. In addition, experimental HOMO and LUMO values were measured *via* cyclic voltammetry. The HOMO values of DMP-BP and DBF-BP were determined from the oxidation peaks and found to be at −4.83 eV and −4.96 eV, respectively (Fig. S8, ESI†). The LUMO values were calculated using the band gap values determined by the absorbance edge and were found to be −2.13 eV and −2.27 eV, respectively. When compared to the HOMO and LUMO levels obtained through AC-2 measurements, they exhibited a consistent trend.

Theoretical calculations

The optimized structures and dihedral angles of the two compounds were calculated using Gaussian density functional theory (DFT), as illustrated in Fig. 3. The DFT calculations were used to investigate the characteristics of the conventional

pyrene core and the newly utilized BP core. In Fig. S9 (ESI†), the HOMO−1, HOMO, LUMO, and LUMO+1 electronic density distributions of the pyrene and BP core were calculated using B3LYP/6-31G(d). The BP core exhibited an electronic distribution almost identical to that of pyrene. By analyzing the determined contribution of the electronic transition, the pyrene chromophore exhibited an oscillator strength of 0.2994 at the absorption wavelength of 321 nm, where the HOMO → LUMO transition was identified as the primary process. The BP core exhibited an oscillator strength of 0.3615 at the absorption wavelength of 331 nm, approximately 1.2 times higher than that of pyrene (Table S1, ESI†). This indicates that while maintaining the electron transition characteristics of the pyrene chromophore, the BP core effectively increased rigidity as expected, resulting in enhanced oscillator strength and consequently higher luminescence efficiency. Fig. 3 illustrates the characteristic changes upon the introduction of various alkyl groups on the phenyl group and when the dibenzofuran group is introduced. The two materials were designed by substituting side groups on both sides of the core to prevent intermolecular packing. To investigate the symmetric molecular structure through bond lengths and angles, relevant values were examined *via* molecular calculations. The dihedral angles at the α and β positions within each molecule exhibited similar values, with DMP-BP showing bond lengths of 1.431 Å and 1.429 Å, while DBF-BP exhibited 1.428 Å and 1.425 Å, indicating a symmetric structure. Upon closer examination, the dihedral angles (α and β positions) between the core and side groups of DMP-BP were calculated at 54.5° and 53.0°, whereas for DBF-BP, they were calculated at 63.6° and 62.1°. It was observed that DBF-BP exhibited approximately a 10° greater twist compared to DMP-BP when DBF was introduced, indicating that such significant steric hindrance could more effectively prevent intermolecular interactions. As shown in Fig. S3, S4 (ESI†) and Table 1, DBF-BP exhibits almost no excimer peak formation with increasing solution concentration, and the FWHM values in the film states align with the optical properties mentioned earlier. The electronic density distribution of the HOMO of both compounds was widely distributed over the BP core and side groups. For DBF-BP, the electron density distribution of the LUMO was more localized to the core due to the stronger electron-donating effect of the dibenzofuran-containing side group compared to DMP-BP. This electron-donating effect of the side group is expected to contribute to the improvement of device efficiency. The calculated band gaps (ΔE_{H-L}) of DMP-BP and DBF-BP were 3.16 eV and 3.17 eV which showed a similar trend to the measured band gaps of 2.70 eV and 2.69 eV for DMP-BP and DBF-BP, respectively (Fig. 3).

Thermal properties

The decomposition temperature (T_d) and glass transition temperature (T_g) of the synthesized materials were determined using thermal gravimetric analysis (TGA) and differential scanning calorimetry (DSC), as illustrated in Fig. 4 and Table S2 (ESI†). The T_d values for 5% weight loss of DMP-BP and DBF-BP were measured at 432 °C and 441 °C. This increase in T_d can be attributed to the introduction of benzofuran side groups, which leads to a higher molecular weight and consequently enhances thermal stability. The observed T_g values for DMP-BP and DBF-BP were 154 °C and 184 °C consistent with the trend observed for T_d. Both DBF-BP and DMP-BP did not exhibit a distinct melting point even when heated up to 300 °C. The high thermal stability, such as T_g values exceeding 150 °C, suggests that these materials can maintain a stable device morphology under the operating temperatures of OLED devices, thus potentially extending the device lifetime.[8]

Electroluminescence properties

To confirm the electroluminescence (EL) properties of the synthesized luminescent materials, they were utilized as dopants in the emitting layer of OLED devices. The OLED device structure was ITO/dipyrazino[2,3-*f*:2′,3′-*h*]quinoxaline-2,3,6,7,10,11-hexacarbo-

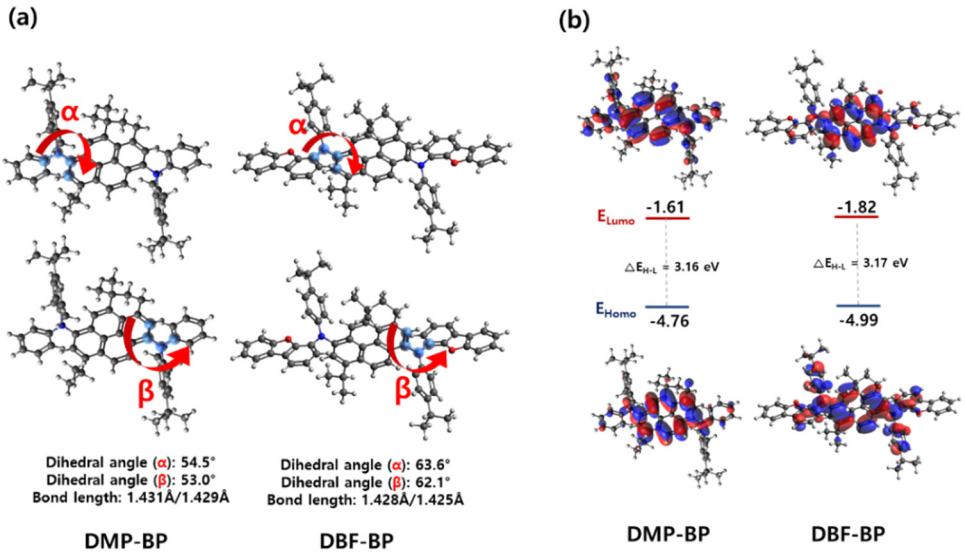

Fig. 3 (a) Both side dihedral angles and bond length of 3*H*-benzo[*c*,*d*]pyrene derivatives and (b) pictorial presentation of the frontier orbitals.

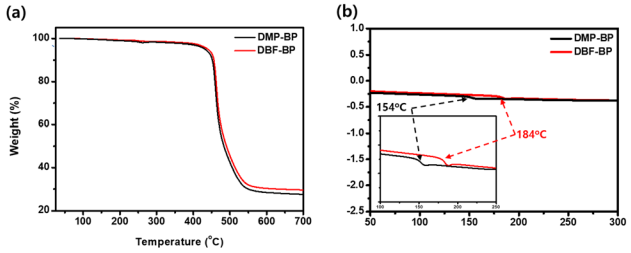

Fig. 4 Thermal properties of DMP-BP and DBF-BP: (a) TGA and (b) DSC (inset: Expansion of the T_g region).

nitrile (HAT-CN) (5 nm)/*N*4,*N*4,*N*4′,*N*4′-tetra[(1,1′-biphenyl)-4-yl]-(1,1′-biphenyl)-4,4′-diamine (BPBPA) (85 nm)/*N*-([1,1′-biphenyl]-4-yl)-*N*-(9,9-dimethyl-9*H*-fluoren-2-yl)spiro[benzo[*de*]anthracene-7,9′-fluoren]-4′-amine (BPACz) (15 nm)/9-(naphthalen-1-yl)-10-(naphthalen-2-*S*-4 yl)anthracene (α,β-ADN: 4% dopant) (25 nm)/DNAPBi and 8-quinolinolato lithium (Liq) (25 nm)/LiF (1 nm)/Al (100 nm). Fig. S10 (ESI†) depicts chemical structures of materials and band diagrams for OLED devices. Fig. 5(a)–(d) illustrates the current density (*J*)–voltage (*V*)–luminance (*L*) curves, current efficiency (CE)–*J*, external quantum efficiency (EQE)–*J*, and device lifetimes of fabricated OLED devices. The EL performance data of the doped devices is summarized in Table 2. The OLED devices utilizing DMP-BP and DBF-BP as dopants exhibited typical *J*–*V*–*L* curves, with turn-on voltages of approximately 3.4 V for both devices. The EL spectra are depicted in Fig. S11 (ESI†), with the EL maximum wavelengths (EL_{max}) of DMP-BP and DBF-BP devices at 463 nm and 459 nm closely resembling the PL maximum wavelength of 457 nm in the solution state. The EL spectra FWHM for DMP-BP and DBF-BP were 44 nm and 42 nm showing narrower values compared to previously reported blue organic light-emitting materials using pyrene cores.[33] The host material for the doped device was α,β-ADN, and we showed the overlap between the PL spectrum of the host material in the film state and the UV absorption spectra of DBP-BP and DBF-BP in solution state, revealing a significant overlapped area. This indicates efficient energy transfer from the host to the dopant (Fig. S12, ESI†). MP-BP emitted a real-blue light with CIE (*x*, *y*) values of (0.138, 0.168), achieving a CE of 9.41 cd A^{-1}, power efficiency (PE) of 6.24 lm W^{-1}, and an EQE of 7.17%. DBF-BP also emitted real-blue light with CIE (*x*, *y*) values of (0.134, 0.139), obtaining a CE of 8.95 cd A^{-1}, PE of 6.08 lm W^{-1}, and an EQE of 7.90% (Fig. 5 and Table 2). At 10 mA cm^{-2}, the luminance values for DMP-BP and DBF-BP were 937 cd m^{-2} and 905 cd m^{-2}, respectively, indicating high brightness levels. Although DBF-BP showed relatively lower CE values compared to DMP-BP, its superior CIE y value led to a high EQE of 7.9%, with a maximum EQE exceeding 8% efficiency.

Additionally, as can be seen in Fig. 5(c), the roll-off in both devices was not large. DBF-BP exhibited a 2.4% roll-off value at 1000 nit relative to the maximum EQE, while DMP-BP showed a 3.3% EQE roll-off value under the same conditions. This indicates that DBF-BP exhibited a more stable roll-off characteristic compared to DMP-BP. The EQE_{max} of OLEDs using DBP-BP and DBF-BP as dopants showed high values of 7.39% and 8.03%, respectively. Considering BP as a core based on the pyrene chromophore with unique photophysical properties and emitter singlet/triplet energy levels, we believe that these high EQE values can be induced by singlet excitons generated in the TTA channel.[34,35] To clarify the cause of high efficiency exceeding 7%, transient EL measurements were performed, and the results are presented in Fig. S13 (ESI†). As shown in the figure, a delayed

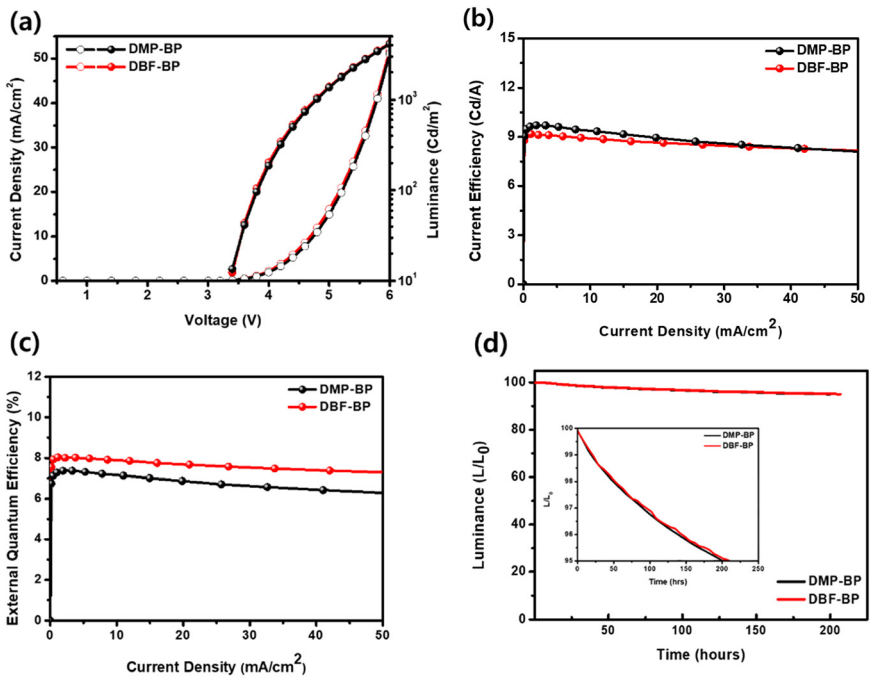

Fig. 5 EL characteristics of devices using DMP-BP and DBF-BP as emitting layer: (a) *J*–*V*–*L* curve, (b) luminance efficiency *versus* current density, (c) external quantum efficiency *versus* current density, and (d) device lifetime of OLED devices (inset: device lifetime LT_{95}).

Table 2 EL performances of the fabricated OLED devices

EMLs	T_{on}[a] (V)	Luminance[b] (cd m^{-2})	CE[b]/CE$_{max}$ (cd A^{-1})	PE[b] (lm W^{-1})	EQE[b]/EQE$_{max}$ (%)	CIE (x, y)[c]	EL$_{max}$ (nm)	FWHM (nm)	LT$_{95}$[d] (h)
DMP-BP	3.4	937	9.41/9.72	6.24	7.17/7.39	(0.138, 0.168)	463	44	202
DBF-BP	3.4	905	8.95/9.15	6.08	7.90/8.03	(0.134, 0.139)	459	42	207

[a] Turn-on voltage at 1 cd m^{-2}. [b] At 10 mA cm^{-2}. [c] Commission International de l'Eclairage. [d] LT$_{95}$ means the device lifetime that final light intensity reaches 95% of initial light intensity (1000 cd m^{-2}).

electroluminescence response was observed, indicating the presence of delayed electroluminescence generated by regenerated singlets, which is interpreted as leading to efficiency enhancement. The stability of the fabricated OLED devices was evaluated by measuring the device lifetime at 1000 cd m^{-2}. The LT$_{95}$ values for DMP-BP and DBF-BP were 202 and 207, respectively, indicating excellent device lifetime exceeding 200 hours (Fig. 5(d)). Here, LT95 represents the device lifetime at which the final luminance reaches 95% of the initial luminance. When calculated for LT$_{50}$, DBF-BP is estimated to have a device lifetime of more than 12 000 hours.[27] DBF-BP demonstrated excellent EL performance with remarkably high CE, PE, and EQE values. It meets the minimum requirements for mobile phone displays, with a CIE y value of 0.139, which is below the threshold of 0.15.

Experimental

Synthetic methods

The core group 1,7-dibromo-9-isopropyl-5,5-dimethyl-4,5-dihydro-3*H*-benzo[*cd*]pyrene and the two side groups, 4-(*tert*-butyl)-2,6-dimethyl-*N*-phenylaniline and *N*-(4-isopropylphenyl)dibenzo[*b*,*d*]-furan-3-amine, were purchased from Material Science Co., Ltd.[36]

Synthesis of N^1,N^7-bis(4-(*tert*-butyl)-2,6-dimethylphenyl)-9-isopropyl-5,5-dimethyl-N^1,N^7-diphenyl-4,5,6*a*1,11*a*1-tetrahydro-3*H*-benzo[*cd*]pyrene-1,7-diamine (DMP-BP)

1,7-Dibromo-9-isopropyl-5,5-dimethyl-4,5-dihydro-3*H*-benzo[*cd*]-pyrene 1.0 g (2.13 mmol), 4-(*tert*-butyl)-2,6-dimethyl-*N*-phenyl-aniline 1.62 g (6.38 mmol), $Pd_2(dba)_3$ 0.097 g (0.106 mmol), sodium *tert*-butoxide 1.23 g (12.7 mmol) and tri-*tert*-butylphosphine 0.05 ml (0.213 mmol) were added to 100 mL of anhydrous toluene in a 3-neck round bottom flask under a N_2 atmosphere. The mixture was refluxed and stirred at 110 °C for 6 h. After the reaction was finished, the mixture was extracted with chloroform and DI water. The organic layer was dried with anhydrous $MgSO_4$ and filtered. The solvent was evaporated. The crude product was purified by column chromatography on silica gel using chloroform : hexane = 1 : 10. (Yield 49%) ^{1}H NMR (400 MHz, DMSO): δ(ppm) 8.07 (d, 1H), 7.87 (d, 1H), 7.75 (s, 1H), 7.42 (s,1H), 7.20–7.06 (m, 9H), 6.83 (s, 1H), 6.77 (s, 1H), 6.56 (d, 2H), 6.42 (d, 2H), 3.87 (t, 1H), 2.61 (t, 2H), 2.01 (d, 12H), 1,77 (t, 2H), 1.29 (d, 18H), 1.19 (s, 6H), 1.16 (d, 6H); HR-MS(EI, m/z): [M+] calc'd for $C_{60}H_{66}N_2$, 814.52; found, 814.5233; elemental analysis calc'd (%) for $C_{60}H_{66}N_2$: C 88.40, H 8.16, N 3.44; found: C 88.34, H 8.17, N 3.50%.

Synthesis of N^1,N^7-bis(dibenzo[*b*,*d*]furan-4-yl)-9-isopropyl-N^1,N^7-bis(4-isopropylphenyl)-5,5-dimethyl-4,5-dihydro-3*H*-benzo[*cd*] pyrene-1,7-diamine (DBF-BP)

1,7-Dibromo-9-isopropyl-5,5-dimethyl-4,5-dihydro-3*H*-benzo[*cd*] pyrene 1.0 g (2.13 mmol), *N*-(4-isopropylphenyl)dibenzo-[*b*,*d*]furan-3-amine 1.92 g (6.38 mmol), $Pd_2(dba)_3$ 0.097 g (0.106 mmol), sodium *tert*-butoxide 1.23 g (12.7 mmol) and tri-*tert*-butylphosphine 0.05 mL (0.213 mmol) were added to 100 mL of anhydrous toluene in a 3-neck round bottom flask under a N_2 atmosphere. The mixture was refluxed at 110 °C for 6 h. After the reaction was finished, the mixture was extracted with chloroform and DI water. The organic layer was dried with anhydrous $MgSO_4$ and filtered. The solvent was evaporated. The crude product was purified by column chromatography on silica gel using chloroform : hexane = 1 : 10. (Yield 54%) ^{1}H NMR (400 MHz, DMSO): δ(ppm) 8.22–8.19 (m, 2H), 8.14–8.11 (m, 3H), 8.05 (s, 1H), 7.90 (t, 3H), 7.69 (s, 1H), 7.49–7.35 (m, 6H), 7.25–7.21 (m, 2H), 7.08–7.01 (m, 6H), 6.69 (d, 2H), 6.61 (d, 2H), 3.91 (t, 1H), 2.61 (t, 2H), 1.98–1.93 (m, 2H), 1.71 (t, 2H), 1.22 (t, 12H), 1.15 (t, 12H); HR-MS(EI, m/z): [M+] calc'd for $C_{66}H_{58}N_2O_2$, 910.45; found,910.4493; elemental analysis calc'd (%) for $C_{66}H_{58}N_2O_2$: C 87.00, H 6.42, N 3.07, O 3.51; found: C 87.35, H 6.45, N 3.09, O 3.47%.

Conclusion

We synthesized two blue light emitters, DMP-BP and DBF-BP, based on a novel core, 3*H*-benzo[*c*,*d*]pyrene, which possesses excellent PLQY. The BP core, designed to be more rigid than the pyrene chromophore, exhibits a higher oscillator strength and incorporates various alkyl groups to effectively prevent intermolecular packing. DMP-BP and DBF-BP, utilizing the BP core, enhances the PLQY and EL efficiency of the emitter by incorporating bulky side groups to prevent intermolecular packing. In the case of DBF-BP, a more bulky side group incorporating dibenzofuran with an electron-donating effect is introduced. Both DMP-BP and DBF-BP exhibited CE$_{max}$ values of 9.72 cd A^{-1} and 9.15 cd A^{-1} with EQE$_{max}$ values of 7.39% and 8.03%, demonstrating excellent EL efficiency. Furthermore, DBF-BP achieved a CIE (x, y) value of (0.134, 0.139), showing real blue emission below 0.15, along with a narrow EL spectrum of 42 nm and an EQE value exceeding 8%, demonstrating outstanding EL characteristics. Lifetime measurements of OLED devices revealed an LT$_{95}$ of 207 hours for DBF-BP, with an expected LT$_{50}$ of over 12 000 hours. This core and side design strategy can be extended to various chromophores, facilitating the development of novel emitters with high efficiency and prolonged device lifetimes on this platform.

Author contributions

Conceptualization, H. K. and Sang. P.; methodology, H. L. and K. L.; validation, H. K. and Sun. P.; formal analysis, Sang. P., Sun. P., and K. L.; investigation, H. K., S. K. and Sang. P.; resources, J. P.; writing – original draft preparation, H. K.; writing – review and editing, H. L. and J. P.; visualization, H. K. and S. K.; supervision, J. P.; project administration, J. P.; funding acquisition, J. P.

Conflicts of interest

There are no conflicts to declare.

Acknowledgements

The core group and side groups used in this study were provided by Material Science Co., Ltd. This work was supported by the GRRC program of Gyeonggi province [(GRRCKYUNGHEE2023-B01), Development of ultra-fine process materials based on the sub-nanometer class for the next-generation semiconductors].

Notes and references

1 A. Endo, M. Ogasawara, A. Takahashi, D. Yokoyama, Y. Kato and C. Adachi, *Adv. Mater.*, 2009, **21**, 4802–4806.
2 K. Goushi, K. Yoshida, K. Sato and C. Adachi, *Nat. Photonics*, 2012, **6**, 253–258.
3 F. C. Chen, Y. Yang, M. E. Thompson and J. Kido, *Appl. Phys. Lett.*, 2002, **80**, 2308–2310.
4 S. Kang, H. Lee, Y. Shim, S. Park and J. Park, *Dyes Pigm.*, 2020, **181**, 108555.
5 M. A. Baldo, D. F. O'Brien, Y. You, A. Shoustikov, S. Sibley, M. E. Thompson and S. R. Forrest, *Nature*, 1998, **395**, 151–154.
6 S. Kim, H. Bae, S. Park, W. Kim, J. Kim, J. Kim, Y. Jung, S. Sul, S. Ihn, C. Noh, S. Kim and Y. You, *Nat. Commun.*, 2018, **9**, 1211.
7 I. Rabelo de Moraes, S. Scholz, B. Luessem and K. Leo, *Appl. Phys. Lett.*, 2011, **99**, 053302.
8 S. Kang, H. Kwon, Y.-J. Pu and J. Park, *Mater. Today Energy*, 2021, **21**, 100706.
9 L. Xianhao, S. Mizhen, X. Lei, W. Runzhe, Z. Huayi, P. Yuyu, Z. Shitong, S. Qikun, X. Shanfeng and Y. Wenjun, *Chem. Sci.*, 2020, **11**, 5058–5065.
10 H. Peng, Z. Wei, L. Wu and X. Li, *Opt. Mater.*, 2020, **101**, 109726.
11 M. Qureshi and M. Sundar, *J. Appl. Phys.*, 2005, **97**, 096101.
12 K. R. Justin Thomas, J. T. Lin, Y.-T. Tao and C.-H. Chuen, *Chem. Mater.*, 2004, **16**, 5437.
13 T. Arakane, M. Funahashi, H. Kuma, K. Fukuoka, K. Ikeda, H. Yamamoto, F. Moriwaki and C. Hosogawa, *Dig. Tech. Pap. – Soc. Inf. Disp. Int. Symp.*, 2006, **37**, 37–40.
14 W. Zilong, S. Shaoxin, Z. Xiangyu, C. Hao, C. Jiajin, M. Dongge, Z. Zujin and Z. T. Ben, *Mater. Chem. Front.*, 2021, **5**, 6978–6986.
15 S. Kang, J. Huh, J. Kim and J. Park, *J. Mater. Chem.*, 2020, **8**, 11168–11176.
16 S. Kang, H. Jung, H. Lee, S. Park, J. Kim and J. Park, *J. Mater. Chem.*, 2019, **7**, 14709–14716.
17 J. E. Anthony, *Angew. Chem., Int. Ed.*, 2008, 47, 452–483.
18 J. Huang, J. Su and H. Tian, *J. Mater. Chem.*, 2012 **22**, 10977.
19 W. L. Jia, T. McCormick, Q. D. Liu, H. Fukutani, M. Motala, R. Y. Wang, Y. Tao and S. N. Wang, *J. Mater. Chem.*, 2004, **14**, 3344–3350.
20 S. Lee, K. Park, C. Joo, J. Lee, J. Lee and Y.-H. Kim, *Dyes Pigm.*, 2016, **128**, 19–25.
21 M. Zhu and C. Yang, *Chem. Soc. Rev.*, 2013, **42**, 4963–4976.
22 T. Figueira-Duarte and K. Müllen, *Chem. Rev.*, 2011, **111**, 7260–7314.
23 Z. Liang, Y. Li, J. Yang, Y. Ren and X. Tao, *Tetrahedron Lett.*, 2011, **52**, 1329–1333.
24 Y. Ge, Y. Wen, H. Liu, T. Lu, Y. Yu, X. Zhang, B. Li, S. Zhang, W. Li and B. Yang, *J. Mater. Chem. C*, 2020, **8**, 11830–11838.
25 D. Chercka, S. Yoo, M. Baumgarten, J. Kim and K. Müllen, *J. Mater. Chem. C*, 2014, **2**, 9083–9086.
26 Y. Ahn, S. Kim, J. Song, W. Yeom, J. Lee and M. Suh, *Dyes Pigm.*, 2022, **205**, 110505.
27 H. Jung, S. Kang, H. Lee, Y.-J. Yu, J. Jeong, J. Song, Y. Jeon and J. Park, *ACS Appl. Mater. Interfaces*, 2018, **10**, 30022–30028.
28 W. Tao, W. Kai, J. Chen, Y. Shi, W. Liu, C. Zheng, Y. Li, J. Yu, X. Oua and X. Zhang, *J. Mater. Chem. C*, 2019, **7**, 4475–4483.
29 N. Cho, J. Lee, O. Kim and S. Hwang, *New J. Chem.*, 2020, **44**, 3868–3873.
30 S. Kim, M. Kim, M. Ahn, K.-M. Lee and K.-R. Wee, *Dyes Pigm.*, 2021, **191**, 109362.
31 H. Jung, H. Shin, S. Kim, J. Kim, B.-K. An, J.-H. Lee, H. Ihee and J. Park, *J. Ind. Eng. Chem.*, 2020, **87**, 213–221.
32 J. Kang, J. Lim and J. Lee, *Mater. Chem. Front.*, 2021, **5**, 7259–7266.
33 S. Zhuang, R. Shangguan, H. Huang, G. Tu, L. Wang and X. Zhu, *Dyes Pigm.*, 2014, **101**, 93–102.
34 T. Shan, Z. Gao, X. Tang, X. He, Y. Gao, J. Li, X. Sun, Y. Liu, H. Liu, B. Ying, P. Lu and Y. Ma, *Dyes Pigm.*, 2017, **142**, 189–197.
35 L. Xing, Z.-L. Zhu, J. Ha, Z. Qiu, Z. Yang, D. Lin, W.-C. Chen, Q. Yang, S. Ji, Y. Hao and C.-S. Lee, *Chem. Eng. J.*, 2021, **421**, 127748.
36 Soon Chang Lee, ORGANIC ELECTROLUMINESCENT ELEMENT. PCT/KR2018/000274, January 5, 2018.